

A Comparison of the Finite Element Method on Shishkin and Gartland-Type Meshes for Convection-Diffusion Problems

H.-G. Roos and T. Skalický

Department of Mathematics,

Technical University Dresden,

Mommsen Straße 13,

01062 Dresden, Germany

A Galerkin finite element discretization of a convection-diffusion boundary value problem is considered on two special types of layer-fitted meshes: Shishkin and Gartland-type meshes. The interpolation and discretization error is estimated for two typical problems with exponential and parabolic boundary layers, respectively. For the Galerkin method we obtain uniform convergence (with respect to the perturbation parameter ε) in the ε -weighted H_1 norm. As well as the previously known result of order $O(H \ln(1/H))$ for Shishkin meshes applied to exponential layers, we show that the order of convergence is of order $O(H)$ in all the other cases considered, where H denotes the mesh diameter. Numerical experiments shows that the Galerkin finite element method sometimes yields significantly better accuracy on Gartland-type meshes than on Shishkin meshes.

1. INTRODUCTION

In the development of modern discretization methods for singularly perturbed problems, there is recently a trend away from methods for general meshes and towards solution-adapted meshes. In this context, a very promising approach was introduced by SHISHKIN [9, 10], where fine equidistant meshes are used within layers. Although some classes of problems, e.g., those containing curved layers, cannot yet be solved satisfactorily by this approach, the analysis of various discretization methods shows that such special meshes are in many respects superior to uniform triangulations of the computational domain. For example, a Galerkin finite element method on Shishkin meshes is uniformly

convergent with respect to the singular perturbation parameter without any stabilization (see [11]). The order of convergence for two-dimensional problems with exponential layers is $O(N^{-1} \ln N)$ in the ε -weighted H_1 norm, where the total number of nodes is proportional to N^2 . This is better than $O(N^{-1/2})$, which is the best result obtained so far for exponentially fitted finite element spaces on equidistant meshes (see [6]).

Despite these promising properties of the Shishkin meshes, their practical application entails some difficulties. These are related, for instance, to the solution of the discrete systems of equations as well as the determination of gradients of the numerical solution. Although Shishkin meshes have some analytic advantages because of their simple piecewise equidistant structure, the investigation of alternative meshes with comparable analytical properties seems to be justified because of the above reasons. In this context, Bakhvalov meshes in particular should be mentioned although up to now few results for them are known in two dimensions (cf. [13]).

In this paper we want to analyze the Galerkin finite element method both for Shishkin meshes and for another type of mesh that is graded in the vicinity of layers. Because the latter look like the meshes analyzed by GARTLAND [4] for a finite difference method, we refer to them as *meshes of Gartland type*.

We consider the convection-diffusion problem

$$\begin{aligned} \mathcal{L}(u) &:= -\varepsilon \Delta u + \mathbf{b} \cdot \nabla u + c u = f && \text{in } \Omega = (0, 1)^2, \\ u &= 0 && \text{on } \Gamma. \end{aligned} \tag{1}$$

ASSUMPTION 1. *In the data of the differential equation (1), we assume that $\varepsilon > 0$ and \mathbf{b} , c and f are sufficiently smooth. Furthermore, let $\|\mathbf{b}\|_{L^\infty(\Omega)} = O(1)$ and $c - (\nabla \cdot \mathbf{b})/2 \geq \bar{c} > 0$.*

A comparison of both types of meshes that we consider is not possible in general for (1) as we lack analytical statements that describe the layers in the exact solution. Consequently we restrict our attention to two simple but important practical cases:

Problem I: Exponential layers

First we consider the boundary value problem (1) with

$$\mathbf{b} = (b_1, b_2) \geq (q\beta_1, q\beta_2) > (0, 0),$$

and some arbitrary $q > 1$ (see Figure 1). In this case, two exponential layers are usually present along the outflow boundary at $x = 1$ and $y = 1$.

Problem II: A parabolic boundary layer

In the second problem that we consider,

$$\mathbf{b} = (b_1, 0) \text{ with } b_1 \geq q\beta_1 > 0.$$

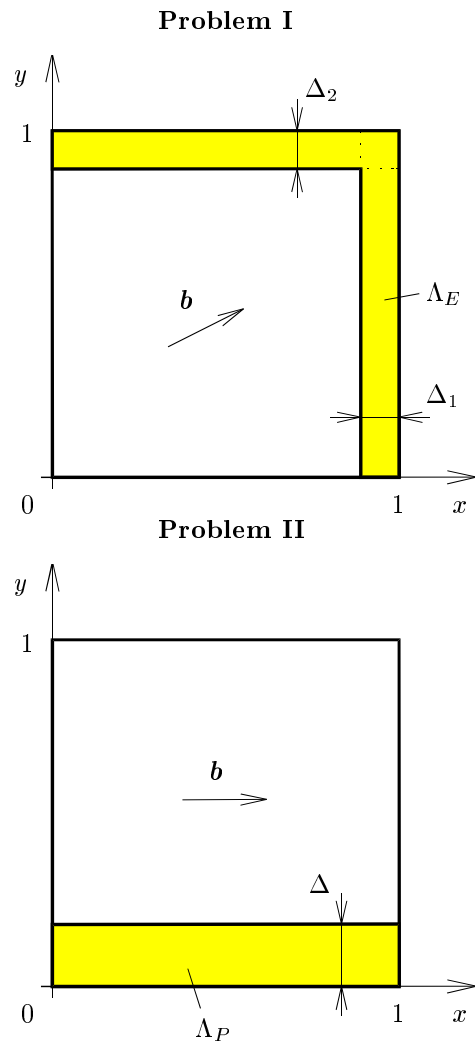


FIGURE 1. Problem statements

We assume that the remaining data in (1) are chosen in such a way that only one parabolic layer arises along the characteristic boundary $y = 0$ (see Figure 1).

The outline of this paper is as follows: we start in Section 2 with a short discussion of the properties of convection-diffusion problems. The focus here is on estimates for the exact solution near exponential and parabolic layers; these are obtained using asymptotic expansions. The Galerkin finite element method is introduced in Section 3 and applied in Sections 4 and 5 to the Shishkin and Gartland-type meshes. Using anisotropic interpolation estimates, we derive

error estimates in the ε -weighted H_1 norm and show that the method is uniformly convergent in all cases. In Section 6 we present some numerical results and quantitatively compare the practical behavior of the Galerkin method on the two types of meshes.

Let us finally remark that our analysis is completely different from the technique used recently in [5] where L_2 -error estimates are proved.

2. PROPERTIES OF THE CONTINUOUS PROBLEM

The construction of layer-adapted grids and the analysis of finite element methods both require information about the behaviour of derivatives of the exact solution. Such information can be obtained heuristically by the formal differentiation of an asymptotic expansion, but it is difficult to provide a solid mathematical foundation for the results obtained (see [8]).

In this chapter we discuss the assumptions that are used in our analysis of finite element methods for Problem I and Problem II.

Problem I: Exponential layers

For Problem I we assume the following:

ASSUMPTION 2. *The solution u of Problem I has the representation*

$$u = G + E_1 + E_2 + E_3, \quad (2)$$

where the smooth part G satisfies

$$\|G\|_{W_\infty^k(\Omega)} \leq C \quad \text{for } k = 0, 1, 2, \quad (3)$$

while the derivatives of the layer terms can be estimated by

$$\left| \frac{\partial^{i+j} E_1}{\partial x^i \partial y^j} \right| \leq C \varepsilon^{-i} \exp\left(-\frac{\beta_1(1-x)}{\varepsilon}\right), \quad (4)$$

$$\left| \frac{\partial^{i+j} E_2}{\partial x^i \partial y^j} \right| \leq C \varepsilon^{-j} \exp\left(-\frac{\beta_2(1-y)}{\varepsilon}\right), \quad (5)$$

$$\left| \frac{\partial^{i+j} E_3}{\partial x^i \partial y^j} \right| \leq C \varepsilon^{-(i+j)} \exp\left(-\frac{\beta_1(1-x)}{\varepsilon}\right) \exp\left(-\frac{\beta_2(1-y)}{\varepsilon}\right) \quad (6)$$

for $i, j = 0, 1, 2$.

Conditions that are sufficient for the existence of such a decomposition are discussed in [3].

Now we denote by Λ_E the subdomain of Ω where layers arise. We shall define Λ_E in such a way that the first-order and second-order derivatives of the exact solution are uniformly bounded in $\Omega \setminus \Lambda_E$. Thus (4) to (6) imply that for the thickness of the layer region we should take

$$\Delta_1 = \frac{2}{\beta_1} \varepsilon \ln(1/\varepsilon), \quad (7)$$

$$\Delta_2 = \frac{2}{\beta_2} \varepsilon \ln(1/\varepsilon); \quad (8)$$

see Figure 1.

Problem II: A parabolic boundary layer

For Problem II we assume, similarly to Problem I, the following:

ASSUMPTION 3. *The solution of Problem 2 admits the representation*

$$u = G + P, \quad (9)$$

where the smooth part G satisfies (3), while the derivatives of the layer term can be estimated by

$$\left| \frac{\partial^{i+j} P}{\partial x^i \partial y^j} \right| \leq C \varepsilon^{-j/2} \exp\left(-\frac{\bar{\beta} y}{\varepsilon^{1/2}}\right) \quad (10)$$

for $i, j = 0, 1, 2$. Here $\bar{\beta}$ is an arbitrary parameter and $C = C(\bar{\beta})$ is a constant that is independent of ε .

We are unaware of any rigorous analysis of conditions sufficient for the existence of such a decomposition for problems with parabolic layers.

The thickness of the layer region Λ_P is now

$$\Delta = \frac{1}{\bar{\beta}} \varepsilon^{1/2} \ln(1/\varepsilon). \quad (11)$$

3. GALERKIN METHOD ON LAYER-FITTED MESHES

The layers arising in Problems I and II are straight and aligned with the axes of the coordinate system, so we shall consider only tensor-product meshes as in Figure 2. We denote the coordinates of the grid lines by $0 = x_0 < x_1 < x_2 < \dots < x_{N_x} = 1$ and $0 = y_0 < y_1 < y_2 < \dots < y_{N_y} = 1$. We handle the layers by using a fine anisotropic mesh. In Problem I this comprises the subdomains Ω_1 , Ω_2 and Ω_3 . We shall use the notation $\Omega_E = \Omega_1 \cup \Omega_2 \cup \Omega_3$ for the entire layer part of Ω . For Problem II, the fine-mesh subdomain is denoted by Ω_P . The width of these subdomains as well as the node distribution depend on the particular type of mesh used. Both these items are discussed in detail in the following Sections. In general, we can assume that $\Omega_E \subseteq \Lambda_E$ and $\Omega_P \subseteq \Lambda_P$, i.e., that $\tau_1 \leq \Delta_1$, $\tau_2 \leq \Delta_2$ and $\tau \leq \Delta$. In the remaining part of Ω_0 , we use a uniform mesh.

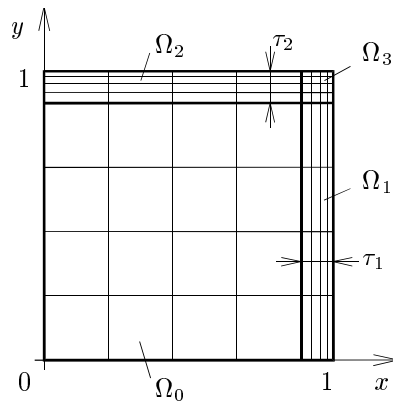
The triangulation of Ω is now defined by

$$\mathcal{T} = \{K = [x_i, x_{i+1}] \times [y_j, y_{j+1}]; 0 \leq i < N_x, 0 \leq j < N_y\}.$$

We use piecewise bilinear functions to approximate the solution. To do this, we introduce the spaces

$$\begin{aligned} V &= H_0^1(\Omega) = \{v \in H^1(\Omega) \mid v = 0 \text{ on } \Gamma\}, \\ V_N &= \{v \in V \mid v \in Q_1(K) \text{ for all } K \in \mathcal{T}\}. \end{aligned}$$

Problem I



Problem II

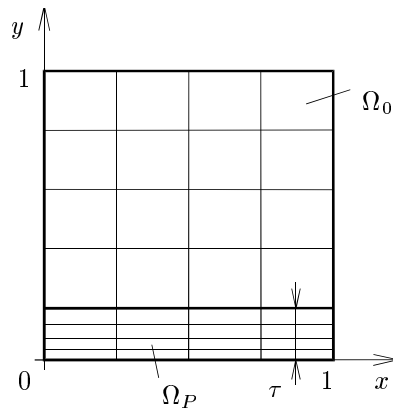


FIGURE 2. Examples of layer-fitted meshes

Then the discrete problem for the Galerkin finite element method can be formulated as follows:

Find $u \in V_N$ such that

$$B(u_N, v_N) = F(v_N) \quad \text{for all } v_N \in V_N, \quad (12)$$

where

$$B(u, v) = \varepsilon (\nabla u, \nabla v) + (\mathbf{b} \cdot \nabla u, v) + (cu, v), \quad (13)$$

$$F(v) = (f, v) \quad (14)$$

for all $u, v \in V$.

The Galerkin orthogonality property

$$B(u_N - u, v_N) = 0 \quad (15)$$

is satisfied by this method. The bilinear form B is V_N -elliptic with

$$B(v_N, v_N) \geq \varepsilon |v_N|_{H^1(\Omega)}^2 + \bar{c} \|v_N\|_{L_2(\Omega)}^2, \quad (16)$$

which follows immediately from integration by parts of the convective term:

$$(\mathbf{b} \cdot \nabla v_N, v_N) = -((v_N, \mathbf{b} \cdot \nabla v_N) + (v_N, (\nabla \cdot \mathbf{b}) v_N)).$$

The ε -weighted H^1 norm

$$\|v_N\|_{\varepsilon, \Omega}^2 := \varepsilon |v_N|_{H^1(\Omega)}^2 + \|v_N\|_{L_2(\Omega)}^2 \quad (17)$$

satisfies the inequality

$$B(v_N, v_N) \geq \gamma \|v_N\|_{\varepsilon, \Omega}^2. \quad (18)$$

The error estimates in the energy norm and in the norm (17) can be reduced to the estimation of the interpolation error $u - u^I$ (we denote the interpolant of $v \in H^2(\Omega)$ in what follows by v^I). The layer-fitted meshes do not satisfy standard regularity assumptions because of the strongly varying mesh size, so we cannot use standard estimates like (see [2])

$$|v - v^I|_{H^k(K)} \leq C \text{diam}(K)^{2-k} |v|_{H^2(K)}, \quad k = 0, 1, 2.$$

Instead, we make use of the following anisotropic relations (see [1]):

LEMMA 1. *Consider a rectangular element $K \in \mathcal{T}$, $K = [x_i, x_{i+1}] \times [y_j, y_{j+1}]$, $0 \leq i < N_x$, $0 \leq j < N_y$. Then for $v \in H^2(K)$ the following interpolation estimates hold:*

$$\begin{aligned} & \|v - v^I\|_{L_\infty(K)} \\ & \leq C \left(h_{x,K}^2 \left\| \frac{\partial^2 v}{\partial x^2} \right\|_{L_\infty(K)} + h_{x,K} h_{y,K} \left\| \frac{\partial^2 v}{\partial x \partial y} \right\|_{L_\infty(K)} + h_{y,K}^2 \left\| \frac{\partial^2 v}{\partial y^2} \right\|_{L_\infty(K)} \right) \end{aligned} \quad (19)$$

$$\begin{aligned} & \|v - v^I\|_{L_2(K)}^2 \\ & \leq C \left(h_{x,K}^4 \left\| \frac{\partial^2 v}{\partial x^2} \right\|_{L_2(K)}^2 + h_{x,K}^2 h_{y,K}^2 \left\| \frac{\partial^2 v}{\partial x \partial y} \right\|_{L_2(K)}^2 + h_{y,K}^4 \left\| \frac{\partial^2 v}{\partial y^2} \right\|_{L_2(K)}^2 \right) \end{aligned} \quad (20)$$

and

$$\left\| \frac{\partial}{\partial x} (v - v^I) \right\|_{L_2(K)}^2 \leq C \left(h_{x,K}^2 \left\| \frac{\partial^2 v}{\partial x^2} \right\|_{L_2(K)}^2 + h_{y,K}^2 \left\| \frac{\partial^2 v}{\partial x \partial y} \right\|_{L_2(K)}^2 \right), \quad (21)$$

$$\left\| \frac{\partial}{\partial y} (v - v^I) \right\|_{L_2(K)}^2 \leq C \left(h_{x,K}^2 \left\| \frac{\partial^2 v}{\partial x \partial y} \right\|_{L_2(K)}^2 + h_{y,K}^2 \left\| \frac{\partial^2 v}{\partial y^2} \right\|_{L_2(K)}^2 \right), \quad (22)$$

where $h_{x,K} = x_{i+1} - x_i$ and $h_{y,K} = y_{j+1} - y_j$.

4. SHISHKIN MESHES

4.1. Node distribution

Let us consider Problem I. We set here $N_x = N_y = N$ and suppose that N is even. The subdomains $\Omega_1, \dots, \Omega_3$ are defined by

$$\tau_1 = \min\{0.5, \frac{2}{\beta_1} \varepsilon \ln N\}, \quad \tau_2 = \min\{0.5, \frac{2}{\beta_2} \varepsilon \ln N\}.$$

We restrict our attention to the convection-dominated case with $\varepsilon \ll N^{-1}$, which is of practical interest; then τ_1 and τ_2 are given by the second arguments in the above formulas. In this case we also have $\ln N \ll \ln(1/\varepsilon)$, so the widths of the subdomains Ω_E and Ω_P on Shishkin meshes are essentially smaller than the widths of the layer regions Λ_E and Λ_P .

Each of the four subdomains has an equidistant mesh of $N/2 \times N/2$ elements. The mesh size in Ω_0 is given by

$$h_{x,K} = \frac{2(1-\tau_1)}{N} \leq \frac{2}{N}, \quad h_{y,K} = \frac{2(1-\tau_2)}{N} \leq \frac{2}{N};$$

in Ω_1 (and analogously in Ω_2 and Ω_3) we obtain

$$h_{x,K} = \frac{2\tau_1}{N} = \frac{4\varepsilon \ln N}{N}, \quad h_{y,K} = \frac{2(1-\tau_2)}{N} \leq \frac{2}{N}.$$

We introduce the mesh size

$$H = \max(h_{x,K}, h_{y,K}) \leq \frac{2}{N}.$$

For Problem II, we set $N_y = 2N_x = N$. The mesh is then defined by

$$\tau = \min\{0.5, \frac{2}{\beta} \varepsilon^{1/2} \ln N\}. \quad (23)$$

In Ω_P we have

$$h_{x,K} = \frac{2}{N} \quad h_{y,K} = \frac{2\tau}{N} = \frac{4\varepsilon^{1/2} \ln N}{N}. \quad (24)$$

The mesh size H can again be bounded by $2/N$.

4.2. The interpolation error

As shown in [3, 11], the following interpolation error estimates are valid for Problem I with exponential layers:

$$\begin{aligned} \|u - u^I\|_{L^\infty(\Omega_0)} &\leq CN^{-2}, \\ \|u - u^I\|_{L^\infty(\Omega_E)} &\leq CN^{-2} \ln^2 N, \end{aligned} \quad (25)$$

$$\begin{aligned} \varepsilon^{1/2} |u - u^I|_{H^1(\Omega_0)} &\leq CN^{-1}, \\ \varepsilon^{1/2} |u - u^I|_{H^1(\Omega_E)} &\leq CN^{-1} \ln N, \end{aligned} \quad (26)$$

and if $\varepsilon^{1/2} \ln^2 N \leq C$, then

$$\|u - u^I\|_{L_2(\Omega)} \leq CN^{-2}. \quad (27)$$

For Problem II, the above inequalities apply mutatis mutandis (one has to replace ε by $\varepsilon^{1/2}$). In particular we have

$$\begin{aligned} \varepsilon^{1/4} \left\| \frac{\partial}{\partial \mathbf{y}} (u - u^I) \right\|_{L_2(\Omega_0)} &\leq CN^{-1}, \\ \varepsilon^{1/4} \left\| \frac{\partial}{\partial \mathbf{y}} (u - u^I) \right\|_{L_2(\Omega_E)} &\leq CN^{-1} \ln N. \end{aligned} \quad (28)$$

On the other hand, assuming that $\varepsilon^{1/2} \ln^2 N \leq C$, we now prove that

$$\left\| \frac{\partial}{\partial x} (u - u^I) \right\|_{L_2(\Omega)} \leq CN^{-1}. \quad (29)$$

This inequality is obviously satisfied by the smooth part $G - G^I$ of the interpolation error, so we need only prove (29) for $P - P^I$.

In Ω_0 , we have

$$\begin{aligned} \left\| \frac{\partial P}{\partial x} \right\|_{L_2(\Omega_0)} &\leq C \exp\left(-\frac{\bar{\beta}\tau}{\varepsilon^{1/2}}\right) \leq CN^{-2}, \\ \|P\|_{L_\infty(\Omega_0)} &\leq C \exp\left(-\frac{\bar{\beta}\tau}{\varepsilon^{1/2}}\right) \leq CN^{-2}, \end{aligned}$$

so an inverse estimate yields

$$\begin{aligned} \left\| \frac{\partial}{\partial x} (P - P^I) \right\|_{L_2(\Omega_0)} &\leq \left\| \frac{\partial P}{\partial x} \right\|_{L_2(\Omega_0)} + \left\| \frac{\partial P^I}{\partial x} \right\|_{L_2(\Omega_0)} \\ &\leq CN^{-2} + CH^{-1} \|P^I\|_{L_2(\Omega_0)} \\ &\leq CN^{-2} + CN \|P^I\|_{L_\infty(\Omega_0)} \\ &\leq CN^{-2} + CN \|P\|_{L_\infty(\Omega_0)} \\ &\leq CN^{-1}. \end{aligned} \quad (30)$$

In Ω_P , we can use the anisotropic estimate (21). Since

$$\left\| \frac{\partial^2 P}{\partial x^2} \right\|_{L_2(\Omega_P)}^2 \leq C, \quad \left\| \frac{\partial^2 P}{\partial x \partial y} \right\|_{L_2(\Omega_P)}^2 \leq C\varepsilon^{-1/2},$$

we invoke the mesh sizes (24) to obtain finally the estimate (29).

4.3. The discretization error

For Problem I, Stynes and O'Riordan [11] derived the error estimate

$$\|u_N - u\|_{\varepsilon, \Omega} \leq CN^{-1} \ln N. \quad (31)$$

We give a brief outline of the proof. The starting point is the ellipticity (18) of the bilinear form B combined with the error orthogonality (15). Applying these to $u_N - u^I$, we obtain

$$\alpha \|u_N - u^I\|_{\varepsilon, \Omega}^2 \leq B(u_N - u^I, u_N - u^I) = B(u - u^I, u_N - u^I).$$

Using integration by parts of the convection term, the bilinear form B can be transformed into

$$B(u, v) = \varepsilon(\nabla u, \nabla v) - (u, \mathbf{b} \cdot \nabla v) + (\tilde{c} u, v),$$

where $\tilde{c} := c - (\nabla \cdot \mathbf{b})$. The diffusion and reaction parts can be estimated using (26) and (27):

$$\begin{aligned} & \left| \varepsilon(\nabla(u - u^I), \nabla(u_N - u^I)) + (\tilde{c}(u - u^I), u_N - u^I) \right| \\ & \leq \varepsilon |u - u^I|_{H^1(\Omega)} |u_N - u^I|_{H^1(\Omega)} \\ & \quad + \|\tilde{c}\|_{L^\infty(\Omega)} \|u - u^I\|_{L_2(\Omega)} \|u_N - u^I\|_{L_2(\Omega)} \\ & \leq \max(1, \|\tilde{c}\|_{L^\infty(\Omega)}) \|u - u^I\|_{\varepsilon, \Omega} \|u_N - u^I\|_{\varepsilon, \Omega} \\ & \leq CN^{-1} \ln N \|u_N - u^I\|_{\varepsilon, \Omega}. \end{aligned} \quad (32)$$

Applying (27) and an inverse estimate, the convection part in Ω_0 is bounded by

$$\begin{aligned} \left| (u - u^I, \mathbf{b} \cdot \nabla(u_N - u^I))_{\Omega_0} \right| & \leq C \|u - u^I\|_{L_2(\Omega_0)} \|\mathbf{b}\|_{L^\infty(\Omega_0)} \\ & \quad H^{-1} \|u_N - u^I\|_{L_2(\Omega_0)} \\ & \leq CN^{-1} \|u_N - u^I\|_{\varepsilon, \Omega_0}. \end{aligned} \quad (33)$$

(The inequality (27) holds true on the subdomain Ω_0 without the hypothesis $\varepsilon^{1/2} \ln^2 N \leq C$.) In Ω_E we have

$$\begin{aligned} \left| (u - u^I, \mathbf{b} \cdot \nabla(u_N - u^I))_{\Omega_E} \right| & \leq \|u - u^I\|_{L^\infty(\Omega_E)} \|\mathbf{b}\|_{L^\infty(\Omega_E)} \|\nabla(u_N - u^I)\|_{L_1(\Omega_E)} \\ & \leq C \|u - u^I\|_{L^\infty(\Omega_E)} (\text{meas } \Omega_E)^{1/2} |u_N - u^I|_{H^1(\Omega_E)}. \end{aligned} \quad (34)$$

From (25) and $(\text{meas } \Omega_E)^{1/2} \leq C\varepsilon^{1/2} \ln^{1/2} N$ it follows that

$$\left| (u - u^I, \mathbf{b} \cdot \nabla(u_N - u^I))_{\Omega_E} \right| \leq CN^{-2} \ln^2 N \ln^{1/2} N \|u_N - u^I\|_{\varepsilon, \Omega_E}. \quad (35)$$

The combination of (32), (33) and (35) yields the estimate (31). \square

For Problem II, we have to modify the Stynes & O'Riordan technique since the transition from (34) to (35) is not possible here as $(\text{meas } \Omega_E)^{1/2} = O(\varepsilon^{1/4})$. Nevertheless, the estimate

$$\begin{aligned} \left| (\mathbf{b} \cdot \nabla(u - u^I), u_N - u^I) \right| & = \left| (b_1 \frac{\partial}{\partial x} (u - u^I), u_N - u^I) \right| \\ & \leq C \left\| \frac{\partial}{\partial x} (u - u^I) \right\|_{L_2(\Omega)} \|u_N - u^I\|_{L_2(\Omega)} \end{aligned} \quad (36)$$

can be applied to the convection term. Then a direct estimate, using (29) and the inequality

$$\begin{aligned} & \left| \varepsilon (\nabla(u - u^I), \nabla(u_N - u)) + (c(u - u^I), u_N - u) \right| \\ & \leq C \|u - u^I\|_{\varepsilon, \Omega} \|u_N - u^I\|_{\varepsilon, \Omega} \\ & \leq C (\varepsilon^{1/4} N^{-1} \ln N + N^{-2}) \|u_N - u^I\|_{\varepsilon, \Omega}, \end{aligned}$$

which is valid for $\varepsilon^{1/2} \ln^2 N \leq C$, leads to the result:

$$\|u_N - u^I\|_{\varepsilon, \Omega} \leq C N^{-1}. \quad (37)$$

Finally, we can formulate the following statement for the parabolic layer problem:

THEOREM 1. *Let assumptions 1 and 3 for Problem II be satisfied and let u_N be the Galerkin approximation of the solution of the given problem using a piecewise bilinear trial space on a Shishkin mesh. If $\varepsilon^{1/2} \ln^2 N \leq C$, then the error estimate (37) is valid.*

REMARK 1. In the case of an exponential layer, if we specify the transition point by the formula $\tau = \tau_0/\beta \cdot \varepsilon \ln N$, then we obtain error terms of the form

$$\tau_0 N^{-1} \ln N + N^{-(\tau_0-1)}.$$

The choice $\tau_0 = 2$ is therefore advisable. This is true also for parabolic layers where the factor 2 in (23) allows a favorable estimate of the layer correction (30).

REMARK 2. For Shishkin meshes the number of nodes is bounded in each direction by

$$H^{-1} \leq N \leq 2 H^{-1}, \quad (38)$$

so the estimate (37) can also be written in the form

$$\|u_N - u^I\|_{\varepsilon, \Omega} \leq C H.$$

Meshes with this property are called meshes of “yoghurt” type in [12]. As we show in the next section, there is no relationship between N and H as simple as (38) for Gartland-type meshes; there the product HN increases (albeit extremely slowly) as ε become smaller (see Section 5.1), so these meshes are not uniformly of “yoghurt” type.

5. GARTLAND-TYPE MESHES

5.1. Node distribution

For meshes of Gartland type, the fine mesh regions Ω_E and Ω_P and the layer parts Λ_E and Λ_P coincide; that is, we choose

$$\tau_1 = \Delta_1, \quad \tau_2 = \Delta_2, \quad \tau = \Delta.$$

The fine subdomains near the layers are therefore essentially wider than in the case of Shishkin meshes.

Outside the layers (i.e., in Ω_0), we use in both Problems a uniform equidistant mesh with $M \times M$ elements. The mesh size can be estimated here by

$$H = \max(h_{x,K}, h_{y,K}) \leq \frac{1}{M}. \quad (39)$$

In the layer parts, the aspect ratio of elements adjacent to the part of the boundary Γ on which exponential or parabolic layers arise is equal to ε and $\varepsilon^{1/2}$, respectively. It is thus of the same order as on Shishkin meshes. But the mesh sizes perpendicular to the layer increase with the distance to Γ until the aspect ratio becomes 1 at the transition to Ω_0 . This guarantees a smooth change of mesh size in the whole domain Ω . Furthermore, the graded distribution of elements in the layer part has a positive effect on the number of nodes used.

For Problem I, we use a distribution of elements in the layer part Ω_1 for which the aspect ratio is defined by

$$\frac{h_{x,K}}{h_{y,K}} = \varepsilon \exp\left(\frac{\beta_1[1-x]_K}{2\varepsilon}\right). \quad (40)$$

Here the distance from the element K to the boundary $x = 1$, at which the layer contained in Ω_1 is located, is denoted by $[1-x]_K$. In Ω_2 , we use an relation analogous to (40). As the asymptotics for the parabolic layer are different, for Problem II in Ω_P we define

$$\frac{h_{y,K}}{h_{x,K}} = \varepsilon^{1/2} \exp\left(\frac{\bar{\beta}[y]_K}{2\varepsilon^{1/2}}\right). \quad (41)$$

A certain optimality of these meshes with respect to the interpolation error of the boundary layer will be discussed in the next section (see Remark 5.2).

REMARK 3. Meshes of this type were first used by Gartland [4] in an analysis of a compact finite-difference method for one-dimensional boundary value problems. The interval $[0, 1]$ was however subdivided by two points

$$x^* = K\varepsilon \ln(K/H), \quad x' = K\varepsilon \ln(1/\varepsilon),$$

which is different from the definition of our mesh. (The parameter K corresponds to the order of the method.) In the so-called inner region $[0, x^*]$ a graded mesh was applied following (40). In the so-called transition region $[x^*, x']$, the mesh sizes were defined by a geometric sequence. Outside these regions an equidistant mesh was used.

Gartland introduced the transition region in order to ensure that the mesh is locally quasi-uniform. This property is not needed in our analysis of the Galerkin method.

The remainder of this section deals with the determination of the number of elements in the layer parts Ω_E and Ω_P . Furthermore, we derive here a

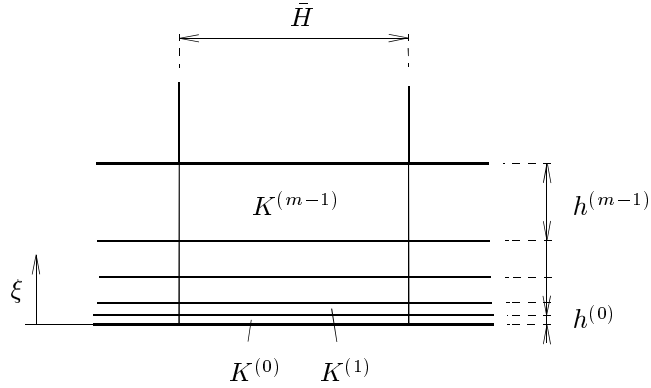


FIGURE 3. Distribution of elements in a layer part

relation between the mesh size H and the total number of elements in Ω . This information is needed in the subsequent error estimates.

The determination of the number of elements m in a layer part in the direction perpendicular to the boundary Γ will follow from relations (40) and (41). In order to simplify the notation, we index the elements beginning from the boundary Γ as shown in Figure 3. For each element $K^{(i)}$, we denote the distance to the boundary by $\xi^{(i)}$ and the “width” of K by $h^{(i)}$. Then the aspect ratio of the element is defined by the recursive formula:

$$\frac{h^{(i)}}{\bar{H}} = \frac{\xi^{(i+1)} - \xi^{(i)}}{\bar{H}} = \varepsilon^\alpha \exp\left(\frac{\beta \xi^{(i)}}{2\varepsilon^\alpha}\right), \quad (42)$$

where

$$0 \leq \xi^{(i)} \leq \Delta = \frac{2\alpha}{\beta} \varepsilon^\alpha \ln(1/\varepsilon).$$

The parameter α depends on the type of the boundary layer: in Ω_1 and Ω_2 we have $\alpha = 1$, while in Ω_P we have $\alpha = 1/2$. In the above formula, the “length” of the elements is denoted by \bar{H} (cf. (40), (41)).

Let us now consider the first $m^* = 2\alpha/(\beta \bar{H}) = (2\alpha/\beta) M$ elements. The mesh size $h^{(i)}$ increases with increasing $\xi^{(i)}$, so for all these elements it is greater than $h^{(0)} = \varepsilon^\alpha \bar{H}$. Hence the width of the first m^* elements exceeds

$$\Delta^* := m^* h^{(0)} = \frac{2\alpha}{\beta} \varepsilon^\alpha.$$

j	$\sum_{i=0}^{j-1} h^{(i)}/\Delta^*$	for	
		$\alpha = 1$	$\alpha = 1/2$
m^*	$> \alpha$	> 1	> 0.5
$2m^*$	$> \alpha e^\alpha$	> 2.7182	> 0.8243
$3m^*$	$> \alpha e^{\alpha e^\alpha}$	> 15.154	> 1.1402
$4m^*$	$> \alpha e^{\alpha e^{\alpha e^\alpha}}$	$> 3.8 \cdot 10^6$	> 1.5637
$5m^*$	\vdots		≥ 2.3882
$6m^*$	\vdots		≥ 5.4472
$7m^*$	\vdots		≥ 116.06
$8m^*$	\vdots		$\geq 1.2 \cdot 10^{50}$

TABLE 1. Total width of j elements within the layer part

The mesh size of the next m^* elements ($m^* \leq i < 2m^*$) is

$$h^{(i)} \geq h^{(m^*)} \geq \varepsilon^\alpha \exp\left(\frac{\beta \Delta^*}{2\varepsilon^\alpha}\right) \bar{H} = \varepsilon^\alpha e^\alpha \bar{H},$$

so the total width of these $2m^*$ elements is at least

$$\Delta^* + m^* h^{(m^*)} = \Delta^* (1 + e^\alpha) \geq \Delta^* e^\alpha.$$

This procedure can be continued. The results are summarized in Table 1.

The width of the layer part equals $\Delta = \Delta^* \ln(1/\varepsilon)$, so one can conclude from the entries in Table 1 that the number of elements perpendicular to the layer is, for practical values of ε , at most $4m^*/\alpha = 8/(\beta \bar{H})$. In order to state this result precisely, we define a function $\lambda_\alpha : \mathbb{N} \rightarrow \mathbb{R}$ by

$$\lambda_\alpha(1) = \alpha, \quad \lambda_\alpha(k+1) = \alpha e^{\lambda_\alpha(k)} \quad \text{for } k \in \mathbb{N},$$

where $n_\alpha(\varepsilon)$ is defined as the greatest positive integer for which

$$\lambda_\alpha(n_\alpha(\varepsilon)) \geq \ln(1/\varepsilon).$$

Then we see that $m \leq n_\alpha(\varepsilon) m^*$. For $\varepsilon \geq 10^{-100000}$ we obviously have $n_\alpha(\varepsilon) \leq 4/\alpha$ and in practice $n_\alpha(\varepsilon)$ can be regarded as bounded.

We can derive a lower bound for m by using the monotonic dependence of the mesh size $h^{(i)}$ on the coordinate $\xi^{(i)}$:

$$\int_0^\Delta \frac{1}{h(\xi)} d\xi \geq \int_0^\Delta \left(\varepsilon^\alpha \bar{H} \exp\left(\frac{\beta \xi}{2\varepsilon^\alpha}\right) \right)^{-1} d\xi = \frac{2}{\beta \bar{H}} (1 - \varepsilon^\alpha).$$

Because of the uniformity of the mesh in Ω_0 , we have

$$\frac{1}{C} H \leq \bar{H} \leq CH.$$

The number of elements m in the layer part is thus bounded by

$$C'(1 - \varepsilon^\alpha) H^{-1} \leq m \leq C'' n_\alpha(\varepsilon) H^{-1}. \quad (43)$$

The total number of elements used in Problem I can therefore be estimated by

$$C'(1 - \varepsilon^\alpha)^2 H^{-2} \leq N_x N_y \leq C''(1 + n_\alpha(\varepsilon))^2 H^{-2} \quad (44)$$

and for Problem II by

$$C'(1 - \varepsilon^\alpha) H^{-2} \leq M N_y \leq C''(1 + n_\alpha(\varepsilon)) H^{-2}. \quad (45)$$

Finally, let us prove the following lemma which plays a role in the interpolation error estimates in the next section.

LEMMA 2. *Let the mesh sizes $h^{(i)}$ be defined by (42). Then the estimate*

$$\sum_{i=0}^m \exp\left(-\frac{\beta \xi^{(i)}}{2\varepsilon^\alpha}\right) \leq C\bar{H}^{-1} \quad (46)$$

is valid.

PROOF. We use the technique already applied in determining the upper bound for m , viz., a step-by-step estimation for sections of m^* elements. We obtain

$$\begin{aligned} \sum_{i=0}^m \exp\left(-\frac{\beta \xi^{(i)}}{2\varepsilon^\alpha}\right) &\leq \sum_{i=0}^{\infty} \exp\left(-\frac{\beta \xi^{(i)}}{2\varepsilon^\alpha}\right) \leq \\ &m^* \left(1 + e^{-\alpha} + e^{-\alpha e^\alpha} + e^{-\alpha e^{\alpha e^\alpha}} + \dots\right). \end{aligned}$$

It can be easily shown that for $\alpha = 1$ and $\alpha = 1/2$ we have

$$\begin{aligned} \left(1 + e^{-\alpha} + e^{-\alpha e^\alpha} + e^{-\alpha e^{\alpha e^\alpha}} + \dots\right) &\leq \frac{1}{\alpha} (1 + e^{-\alpha} + e^{-2\alpha} + e^{-3\alpha} + \dots) \\ &\leq \frac{1}{\alpha} \frac{1}{1 - e^{-\alpha}} \leq \frac{3}{\alpha}. \end{aligned}$$

Consequently,

$$\sum_{i=0}^m \exp\left(-\frac{\beta \xi^{(i)}}{2\varepsilon^\alpha}\right) \leq \frac{2m^*}{\alpha} \leq \frac{6}{\beta\bar{H}} \leq C\bar{H}^{-1}$$

is also valid. □

5.2. The interpolation error

In this section, we derive interpolation error estimates for Gartland-type meshes that are analogous to those of Section 4.2.

THEOREM 2. For Problem I, the interpolation error satisfies

$$\|u - u^I\|_{L_\infty(\Omega)} \leq CH^2, \quad (47)$$

$$\begin{aligned} |u - u^I|_{H^1(\Omega_0)} &\leq CH, \\ \varepsilon^{1/2} |u - u^I|_{H^1(\Omega_E)} &\leq CH, \end{aligned} \quad (48)$$

$$\|u - u^I\|_{L_2(D)} \leq CH^2 (\text{meas } D)^{1/2}, \quad (49)$$

where $D \subset \Omega$.

For Problem II, the estimates (47) and (49) remain valid. Instead of (48), we have

$$\begin{aligned} |u - u^I|_{H^1(\Omega_0)} &\leq CH, \\ \varepsilon^{1/4} |u - u^I|_{H^1(\Omega_P)} &\leq CH \end{aligned} \quad (50)$$

and in particular

$$\left\| \frac{\partial}{\partial x} (u - u^I) \right\|_{L_2(\Omega)} \leq CH. \quad (51)$$

PROOF. The starting point for the proof of the interpolation estimates is, as for Shishkin meshes, the decompositions (2) and (9). Let us first consider Problem I and the interpolation error in the L_∞ norm. The exact solution u is bounded in Ω_0 , so the standard estimate

$$\|u - u^I\|_{L_\infty(\Omega_0)} \leq CH^2$$

can be applied here. In Ω_1 , the inequality (19) is satisfied in each element K . Taking into account (40) and (4) or

$$\left\| \frac{\partial^2 E_1}{\partial x^i \partial y^{2-i}} \right\|_{L_\infty(K)} \leq C \varepsilon^{-i} \exp\left(-\frac{\beta_1 [1-x]_K}{\varepsilon}\right) \quad \text{for } i = 0, 1, 2,$$

we obtain immediately

$$\|E_1 - E_1^I\|_{L_\infty(\Omega_1)} \leq CH^2.$$

Because $G + E_2 + E_3$ is bounded in Ω_1 , the inequality

$$\|u - u^I\|_{L_\infty(\Omega_1)} \leq CH^2 \quad (52)$$

is also satisfied. Analogous results for the subdomains Ω_2 and Ω_3 finally yield (47).

Let us now consider the interpolation error in the ε -weighted H_1 seminorm. Standard estimates remain valid in Ω_0 . It can be easily shown that, for each element in Ω_1 , $\frac{\partial}{\partial x} (E_1 - E_1^I)$ is the dominant derivative of the gradient in the decomposition (2). According to (4), we have

$$\begin{aligned} \left\| \frac{\partial^2 E_1}{\partial x^2} \right\|_{L_2(K)}^2 &\leq C \varepsilon^{-4} \exp\left(-\frac{2\beta_1 [1-x]_K}{\varepsilon}\right) h_{x,K} H, \\ \left\| \frac{\partial^2 E_1}{\partial x \partial y} \right\|_{L_2(K)}^2 &\leq C \varepsilon^{-2} \exp\left(-\frac{2\beta_1 [1-x]_K}{\varepsilon}\right) h_{x,K} H. \end{aligned}$$

Then the anisotropic interpolation estimate (21) and the aspect ratio (40) for the element K together yield

$$\left\| \frac{\partial}{\partial x} (E_1 - E_1^I) \right\|_{L_2(K)}^2 \leq C \varepsilon^{-1} \exp \left(-\frac{\beta_1 [1-x]_K}{2\varepsilon} \right) H^4.$$

Summing over all elements of Ω_1 and using (46), we obtain

$$\varepsilon^{1/2} \left\| \frac{\partial}{\partial x} (E_1 - E_1^I) \right\|_{L_2(\Omega_1)} \leq CH,$$

so

$$\varepsilon^{1/2} |u - u^I|_{H^1(\Omega_1)} \leq CH$$

is also true. Analogous estimates for Ω_2 and Ω_3 result in (48).

The estimate of the interpolation error in the L_2 norm can be done in the same way. For example, let us consider again the boundary layer correction E_1 in the subdomain Ω_1 . We have here

$$\|E_1 - E_1^I\|_{L_2(K)}^2 \leq C (\text{meas } K) H^4.$$

The sum over all elements yields

$$\|u - u^I\|_{L_2(\Omega_1)} \leq C (\text{meas } \Omega_1)^{1/2} H^2.$$

Thus (49) is valid.

The proofs of (47) and (49) for Problem II are analogous to those for Problem I, and the inequality (50) can be derived analogously to (48). The differences in the ε -weighting can be explained by the different asymptotics of the parabolic layer (i.e., now $\alpha = 1/2$).

For (51), we can start from the fact that u is bounded in Ω_0 ; then (51) is just a standard estimate. In Ω_P we have

$$\left\| \frac{\partial^2 P}{\partial x^2} \right\|_{L_2(K)}^2 \leq C h_{y,K} H, \quad \left\| \frac{\partial^2 P}{\partial x \partial y} \right\|_{L_2(K)}^2 \leq C \varepsilon^{-1} \exp \left(-\frac{2\bar{\beta} [y]_K}{\varepsilon} \right) h_{y,K} H.$$

On each element K , the anisotropic estimate (21) yields

$$\left\| \frac{\partial}{\partial x} (u - u^I) \right\|_{L_2(K)} \leq C \left(H^2 + \varepsilon^{-1} \exp \left(-\frac{2\bar{\beta} [y]_K}{\varepsilon} \right) h_{y,K}^2 \right) h_{y,K} H \leq C h_{y,K} H^3.$$

Hence the sum over all elements in Ω_P leads to

$$\left\| \frac{\partial}{\partial x} (u - u^I) \right\|_{L_2(\Omega_P)} \leq C \varepsilon \ln(1/\varepsilon) H^2 \leq CH^2$$

and (51) is therefore satisfied. \square

REMARK 4. It can be shown easily that the estimate (47) is valid not only globally but is also sharp with respect to an arbitrary element $K \in \mathcal{T}$. In this case, the constant C depends on neither the form (aspect ratio) of the element nor on the parameter ε . This attractive property motivated us to investigate such graded meshes in detail. Only afterwards did we discover a resemblance to the meshes used by Gartland.

5.3. The discretization error

We use the same technique as in Section 4.3 for the proof of the error estimate. In the ε -weighted H_1 norm, we have as a starting point

$$\alpha \|u_N - u^I\|_{\varepsilon, \Omega}^2 \leq C \|u - u^I\|_{\varepsilon, \Omega} \|u_N - u^I\|_{\varepsilon, \Omega} + |(u - u^I, \mathbf{b} \cdot \nabla(u_N - u^I))|.$$

For the convection term, it follows from (49) that in Ω_E we have

$$\begin{aligned} |(u - u^I, \mathbf{b} \cdot \nabla(u_N - u^I))_{\Omega_E}| &\leq \varepsilon^{-1/2} \|u - u^I\|_{L_2(\Omega_E)} \varepsilon^{1/2} |u_N - u^I|_{H_1(\Omega_E)} \\ &\leq CH^2 \ln(1/\varepsilon) \|u_N - u^I\|_{\varepsilon, \Omega_E}. \end{aligned}$$

In Ω_0 , using an inverse estimate, we obtain

$$\begin{aligned} |(u - u^I, \mathbf{b} \cdot \nabla(u_N - u^I))_{\Omega_0}| &\leq \|u - u^I\|_{L_2(\Omega_0)} H^{-1} \|u_N - u^I\|_{L_2(\Omega_0)} \\ &\leq CH \|u_N - u^I\|_{\varepsilon, \Omega_0}. \end{aligned}$$

Obviously

$$\|u - u^I\|_{\varepsilon, \Omega} \leq CH$$

is satisfied. This yields immediately

$$\|u_N - u^I\|_{\varepsilon, \Omega} \leq CH. \quad (53)$$

Considering Problem II, we take the convection term in its original form, which leads to

$$\alpha \|u_N - u^I\|_{\varepsilon, \Omega}^2 \leq C \|u - u^I\|_{\varepsilon, \Omega} \|u_N - u^I\|_{\varepsilon, \Omega} + |(\mathbf{b} \cdot \nabla(u - u^I), u_N - u^I)|.$$

While

$$\|u - u^I\|_{\varepsilon, \Omega} \leq C \left(\varepsilon^{1/4} H + H^2 \right),$$

the convection term yields (using (51) in (36))

$$|(\mathbf{b} \cdot \nabla(u - u^I), u_N - u^I)| \leq CH \|u_N - u^I\|_{\varepsilon, \Omega}.$$

Altogether, we obtain the estimate (53) for Problem II with a parabolic layer.

The results are summarized in the following statement.

THEOREM 3. *Let the assumptions 1, 2 and 3 for Problem I and II be satisfied and let u_N be the Galerkin approximation of the solution of the given problems using a piecewise bilinear trial space on a Gartland-type mesh. Then the error estimate (53) is valid.*

6. NUMERICAL RESULTS

In this section, we verify that our error estimates hold true numerically for some examples. In particular, we are interested in seeing whether or not there are quantitative differences between the practical convergence behaviour of the Galerkin method on Shishkin and Gartland-type meshes.

The first test problem is of type I. The coefficients of the differential equation (1) are

$$\mathbf{b} = \begin{pmatrix} 3-y \\ 3-x \end{pmatrix}, \quad c = 0, \quad f = x(3-x) + y(3-y).$$

Homogeneous Dirichlet boundary conditions are given on the whole boundary, so exponential layers appear along $x = 1$ and $y = 1$ (see Figure 4). Far from

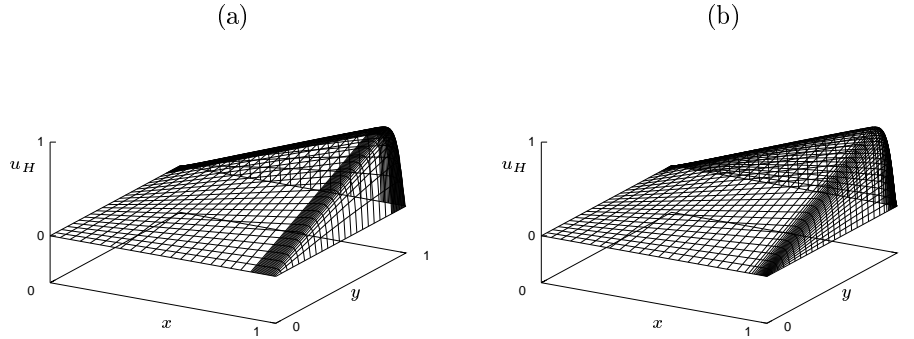


FIGURE 4. Example I: A numerical solution of for $\varepsilon = 3 \cdot 10^{-2}$ on a Shishkin (a) and a Gartland-type (b) mesh

the layers, the exact solution converges to the solution of the reduced problem $u_0 = xy$ as $\varepsilon \rightarrow 0$.

The second test problem is defined by

$$\mathbf{b} = \begin{pmatrix} 1 \\ 0 \end{pmatrix}, \quad c = 0, \quad f = 0.$$

The boundary conditions are

$$\begin{aligned} u &= 0 && \text{at } x = 0, \\ u &= \exp\left(4 - \frac{1}{x(1-x)}\right) && \text{at } y = 0, \\ \mathbf{n} \cdot \nabla u &= 0 && \text{at } x = 1 \text{ and } y = 1. \end{aligned}$$

In this case there is a parabolic layer along the boundary $y = 0$ (see Figure 5). The derivatives of the exponential function that describes the solution on the boundary vanish at $x = 0$ and $x = 1$. Our numerical tests have shown that this property guarantees that no oscillations appear in the discrete solution at the corners $(0,0)$ and $(1,0)$ of Ω . In other cases, corner singularities arise.

The meshes described in the previous sections for Problem II do not however avoid a weak layer at $x = 1$. The corresponding layer correction (we denote it by E') in the asymptotic expansion of the exact solution can be estimated by an inequality of the type

$$\left| \frac{\partial^{i+j} E'}{\partial x^i \partial y^j} \right| \leq C \varepsilon^{1-i} \exp\left(-\frac{\beta_1(1-x)}{\varepsilon}\right).$$

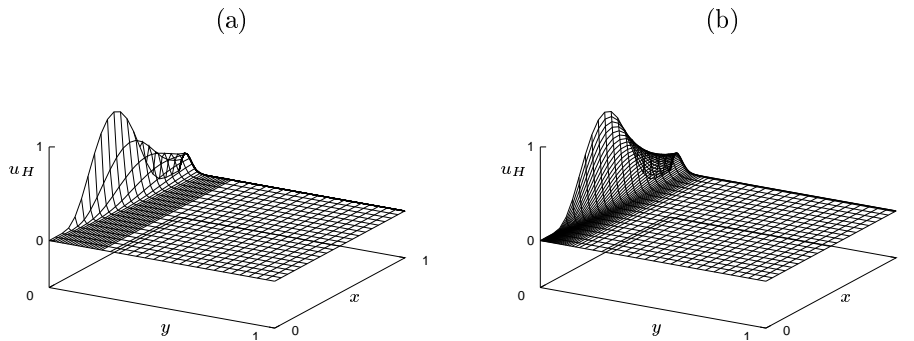


FIGURE 5. Example II: A numerical solution of for $\varepsilon = 10^{-3}$ on a Shishkin (a) and a Gartland-type (b) mesh

The width of the layer part is then equal to

$$\Delta' = \frac{1}{\beta_1} \varepsilon \ln(1/\varepsilon).$$

In order to approximate the solution as exactly as possible, we introduce a fine mesh on a strip in the vicinity of the outflow boundary. For the Shishkin mesh, we set

$$\tau' = \frac{1}{\beta_1} \varepsilon \ln N,$$

subdivide Ω by the lines $x = 1 - \tau'$ and $y = 1 - \tau$ (see (23)) and define the triangulation in each of these subdomains by a equidistant mesh consisting of $N/2 \times N/2$ elements. The modification of the Gartland-type mesh is a little more complicated. In this case we apply a graded mesh near the boundary $x = 1$. It is constructed in such a way that the aspect ratio of the elements is equal to

$$\frac{h_{x,K}}{h_{y,K}} = \varepsilon^{1/2} \exp\left(\frac{\beta_1[1-x]_K}{2\varepsilon}\right).$$

For further details see [7].

The Galerkin finite element method has been proved to be uniformly convergent in the ε -weighted norm for both types of meshes considered. This pleasant property does not inevitably mean, however, that the resulting algebraic systems of equations are easy to solve. In fact, no robust convergence behavior could be established with standard iterative methods for non-symmetric systems such as GMRES or BiCGSTAB. In order to avoid the use of direct solvers, we have applied the following defect correction method:

$$\begin{aligned} B_{GLS}(u_N^{(0)}, v_N) &= F(v_N), \\ B_{GLS}(u_N^{(i+1)} - u_N^{(i)}, v_N) &= F(v_N) - B(u_N^{(i)}, v_N), \quad i = 1, 2, \dots \end{aligned}$$

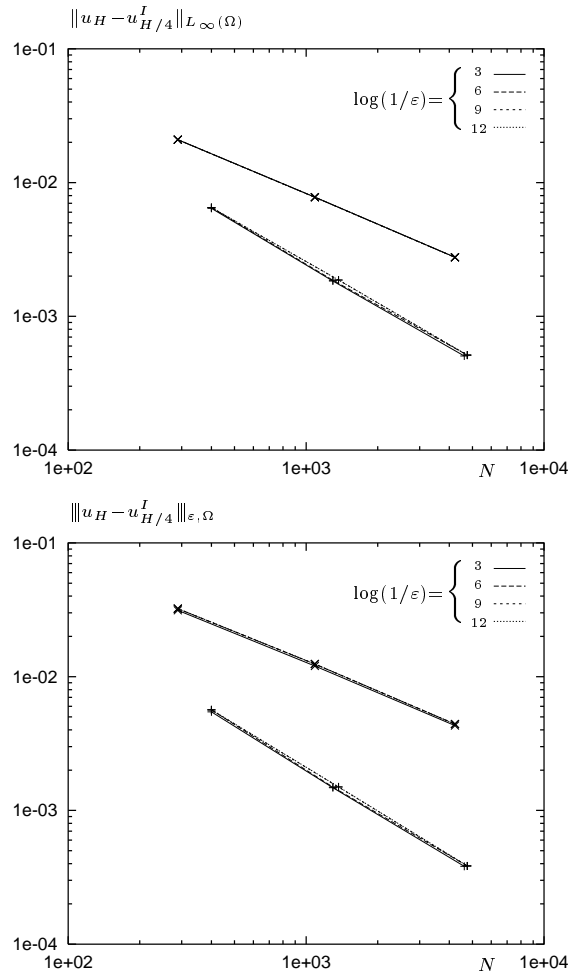


FIGURE 6. Example I: Convergence behavior on a Shishkin (×) and a Gartland-type (+) mesh

The bilinear form B_{GLS} corresponds to the Galerkin/least-squares finite element method which was analyzed for Gartland-type meshes in [7]. The systems of equations obtained by this stable discretization can be solved by standard iterative methods. We find that a combination of the BiCGSTAB method and SSOR preconditioning is quite efficient for Problem I. On the other hand, GMRES(20) seems to be more suitable for Problem II. The stopping criterion for both solvers was defined in such a way that the error of the iterative solution can be neglected in comparison with the discretization error.

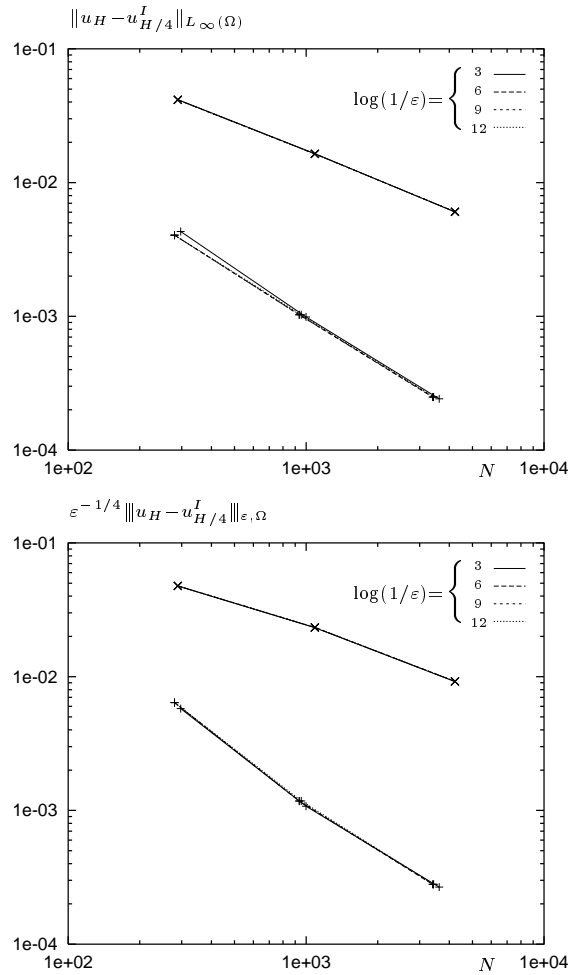


FIGURE 7. Example II: Convergence behavior on a Shishkin (x) and a Gartland-type (+) mesh

The discretization error was computed in our numerical experiments using the so-called “double-mesh principle”, but we discovered that a fine mesh generated by bisection of mesh size of the original mesh was not fine enough for a precise approximation of the exact solution. Consequently we applied double refinements in constructing the refined mesh. The discretization error was then computed as the difference between the discrete solution u_H obtained on the original mesh and the solution $u_{H/4}^I$ from the refined mesh, where the solution $u_{H/4}^I$ was projected into the trial space of the original mesh.

Shishkin mesh

H	$N_x N_y$	$\ u_H - u_{H/4}^I\ _{L_\infty(\Omega)}$	r	$\ u_H - u_{H/4}^I\ _{\varepsilon,\Omega}$	r
1.25000e-01	289	2.09189e-02		3.22660e-02	
6.24998e-02	1089	7.76954e-03	1.429	1.24263e-02	1.377
3.12499e-02	4225	2.76319e-03	1.491	4.42256e-03	1.490

Gartland-type mesh

H	$N_x N_y$	$\ u_H - u_{H/4}^I\ _{L_\infty(\Omega)}$	r	$\ u_H - u_{H/4}^I\ _{\varepsilon,\Omega}$	r
1.24992e-01	400	6.50098e-03		5.64876e-03	
6.24988e-02	1296	1.86233e-03	1.804	1.49592e-03	1.917
3.12154e-02	4761	5.13312e-04	1.859	3.84282e-04	1.961

TABLE 2. Example I: Discretization error for $\varepsilon = 10^{-6}$

Shishkin mesh

H	$N_x N_y$	$\ u_H - u_{H/4}^I\ _{L_\infty(\Omega)}$	r	$\ u_H - u_{H/4}^I\ _{\varepsilon,\Omega}$	r
1.25000e-01	289	4.15236e-02		1.50869e-03	
6.24998e-02	1089	1.63759e-02	1.342	7.37105e-04	1.033
3.12499e-02	4225	6.05049e-03	1.437	2.91423e-04	1.339

Gartland-type mesh

H	$N_x N_y$	$\ u_H - u_{H/4}^I\ _{L_\infty(\Omega)}$	r	$\ u_H - u_{H/4}^I\ _{\varepsilon,\Omega}$	r
1.24985e-01	280	4.04809e-03		2.02225e-04	
6.24961e-02	936	1.02648e-03	1.980	3.71923e-05	2.443
3.12490e-02	3400	2.49348e-04	2.041	8.85457e-06	2.071

TABLE 3. Example II: Discretization error for $\varepsilon = 10^{-6}$

We have analyzed the error in the L_∞ norm and the ε -weighted H_1 norm. Results for $\varepsilon = 10^{-6}$ and various mesh sizes H as well as the numerical convergence rates

$$r = \frac{1}{\ln 2} \ln \left(\frac{\|u_H - u_{H/4}^I\|_{\infty,\Omega}}{\|u_{2H} - u_{H/2}^I\|_{\infty,\Omega}} \right) \quad \text{and} \quad r = \frac{1}{\ln 2} \ln \left(\frac{\|u_H - u_{H/4}^I\|_{\varepsilon,\Omega}}{\|u_{2H} - u_{H/2}^I\|_{\varepsilon,\Omega}} \right)$$

are listed in Tables 2 and 3.

In our numerical tests, we have also verified that the Galerkin method is in practice uniformly convergent with respect to the parameter ε . The convergence behaviour for $\varepsilon = 10^{-3}$, 10^{-6} , 10^{-9} and 10^{-12} shown in graphs in Figures 6 and 7 confirms this property.

REFERENCES

1. T. APEL and M. DOBROWOLSKI (1992). Anisotropic interpolation with applications to the finite element method. *Computing* **47**, 277–293.
2. P. G. CIARLET (1978). *The Finite Element Method for Elliptic Problems*. Studies in mathematics and its applications. North-Holland, Amsterdam.

3. M. Dobrowolski and H.-G. ROOS (1997). A priori estimates for the solution of convection-diffusion problems and interpolation on Shishkin meshes, *Zeitschrift für Analysis und Anwendungen* **16**(4), 1001–1012.
4. E. C. GARTLAND, JR. (1988). Graded-mesh difference schemes for singularly perturbed two-point boundary value problems. *Mathematics of Computation*. **51** (184), 631–657.
5. J. LI and I. M. NAVON (1997). *Uniformly convergent finite element methods for singularly perturbed boundary value problems: convection-diffusion type*. Technical report, Department of Mathematics, Florida State University, July.
6. H.-G. ROOS, D. ADAM and A. FELGENHAUER (1996). A novel nonconforming uniformly convergent finite element method in two dimensions. *Journal of Mathematical Analysis and Applications* **201**, 715–755.
7. H.-G. ROOS and T. SKALICKÝ. *Galerkin/least-squares finite element method for convection-dominated problems on Gartland-type meshes*, Preprint, Dresden University of Technology. (In preparation).
8. H.-G. ROOS, M. STYNES and L. TOBISKA (1996). *Numerical Methods for Singularly Perturbed Differential Equations*. Springer Series in Computational Mathematics. Springer-Verlag, Berlin.
9. G. I. SHISHKIN (1990). *Grid approximation of singularly perturbed elliptic and parabolic equations*, Second doctoral thesis, Keldysh Institute, Russian Academy of Science, Moscow (In Russian).
10. G. I. SHISHKIN (1992). *Discrete approximation of singularly perturbed elliptic and parabolic equations*, Technical report, Ural branch of the Russian Academy of Science, Jekatarinenburg (In Russian).
11. M. STYNES and E. O’RIORDAN (1997). A uniformly convergent Galerkin method of a Shishkin mesh for a convection-diffusion problem. *Journal of Mathematical Analysis and Applications* **214**(1), 36–54.
12. P. M. SELWOOD and A. J. WATHEN (1996). Convergence rates and classification for one-dimensional finite-element-meshes. *IMA Journal of Numerical Analysis* **16**, 65–74.
13. R. VULANOVIĆ (1991). Non-equidistant finite difference methods for elliptic singular perturbation problems. J. J. H. MILLER, editor, *Computational methods for boundary and interior layers in several dimensions*. 203–223, Dublin, Boole press.